Palladian gold from the Cauê iron mine, Itabira District, Minas Gerais, Brazil

G. R. Olivo, M. Gauthier and M. Bardoux

Université du Québec à Montréal, Département des sciences de la terre, case postale 8888, succ. A, Montréal, PQ, Canada, H3C 3P8

Abstract

Palladian gold from the Cauê iron mine, Itabira District, Minas Gerais, Brazil is found in horizons of hydrothermally-altered Lake Superior-type oxide-facies iron-formation locally called jacutinga. Palladium content of the gold grains varies from 1% to 20%, high palladium values being associated with palladium-copper-oxide inclusions and showing island-mainland and replacement (relict) textures in the Corpo Y and Corpo X orebodies. In the Aba Leste orebody, palladium is homogeneously distributed throughout the gold grains.

Palladium and gold mineralization was synchronous with intense D1 shearing. Palladium was deposited early during the generation of S1-mylonitic foliation, and was replaced by gold during progressive deformation.

At high oxygen fugacities (hematite stability field) and high temperatures (up to 600°C), Pd and Au may have been transported as chloride complexes, and their deposition may have occurred mainly as a result of changes in pH, but dilution of Cl concentrations may have also caused Pd and Au precipitation. Deposition of Pd as selenide may have taken place early during the creation of S1-fabrics.

Keywords: gold, palladium, Itabira, Brazil, iron-formation, jacutinga.

Introduction

It is known that some native gold and gold-copper alloys contain palladium (Cabri, 1981). This relationship has been documented for samples from the Stillwater Complex, Montana, United States (Cabri and Laflamme, 1974), the Lac des Iles deposit, Ontario, Canada (Cabri and Laflamme, 1979), the Noril'sk and Talnakh deposits, Russia (Cabri, 1981), Hope's Nose, in Devon, England (Clark and Criddle, 1982); and in Brazil from the Serra Pelada deposit, in Pará State (Meireles and Silva, 1988), and the Congo Soco and Maquiné mines (Bensusan, 1929), the Taquaril and Porpez showings (Cabri, 1981), and the Cauê and Conceiçao mines (Leao de Sá and Borges, 1991; Olivo and Gauthier, 1993; Olivo *et al.*, 1993), all in Minas Gerais State.

The palladian gold occurrences in Minas Gerais, Brazil, discussed in this paper are commonly associated with jacutinga, a hydrothermally-altered Lake Superior-type oxide-facies iron-formation (Bensusan, 1929; Dorr and Barbosa, 1963; Polônia and Souza, 1988; Ladeira, 1991; Leao de Sá and Borges, 1991; Olivo and Gauthier, 1993; Olivo *et al.*, 1993). Despite the fact that the Minas Gerais deposits have been mined since the eighteenth century, the composition and textures of their palladian gold have not been studied in detail. Although most of these mines are presently inactive, gold and palladium are still mined as by-products in the Cauê and occasionally in the Conceiçao iron mines (both mines, separated by approximately 7 km, are located in the Itabira Iron District). In the Conceiçao mine, palladium contents in gold grains are distinctly lower than at the Cauê mine (Leao de Sá and Borges, 1991).

Palladium-bearing high-grade gold ore of the Cauê mine provides a rare opportunity to study textures and compositions of palladian gold in primary ore. In this paper textural details and analytical data for palladian gold from the Cauê mine are reported and discussed in terms of the genesis of this special type of mineralization.

Mineralogical Magazine, December 1994, Vol. 58, pp. 579–587

Cauê iron mine

Geologic units

At the Cauê mine, four geologic units metamorphosed to amphibolite facies have been identified (Fig. 1, Olivo *et al.*, in preparation): (1) a volcano-sedimentary sequence correlated with the Archean Rio das Velhas Supergroup; (2) an iron-formation unit comprised of itabirite (e.g. metamorphosed banded siliceous ironstone consisting of interlayered quartz-hematite-magnetite), massive hematite, and jacutinga which is part of the Early Proterozoic, Lake Superior-type iron-formation of the Itabira Group, Minas Supergroup; (3) a quartzite unit, correlated with the Early Proterozoic Piracicaba Group, Minas Supergroup; and (4) mafic intrusive rocks.

Structure

These rocks were affected by three phases of folding, as well as boudinage and reverse and thrust faulting (Olivo *et al.*, in preparation). D1-structures are represented by tight and isoclinal folds becoming sheath folds where the ENE elongation lineation (Le) and mylonitic foliation (S1) are well developed. D2-structures also include tight folds with associated parasitic fold axes and a transposing foliation (S2).

D3 structures are characterized by open folds with an associated crenulation cleavage.

Millimetric to decametric boudins occur in S1 or S2 foliation planes. Reverse and thrust faults created imbricated sheets that are interpreted as synchronous with D1 deformation. Reactivation of these faults occurred during D2 deformation.

Gold orebodies

To date, five gold orebodies have been mined in the Cauê mine: Corpo Y, Corpo X, Central, Aba Leste, and Aba Norte (Fig.1, Olivo *et al.*, in preparation). All orebodies are hosted by jacutinga. High gold grades (up to 1000 g/t) are associated with quartz- and hematite-rich bands parallel to the S1 mylonitic foliation and/or stretched parallel to the ENE elongation linea-

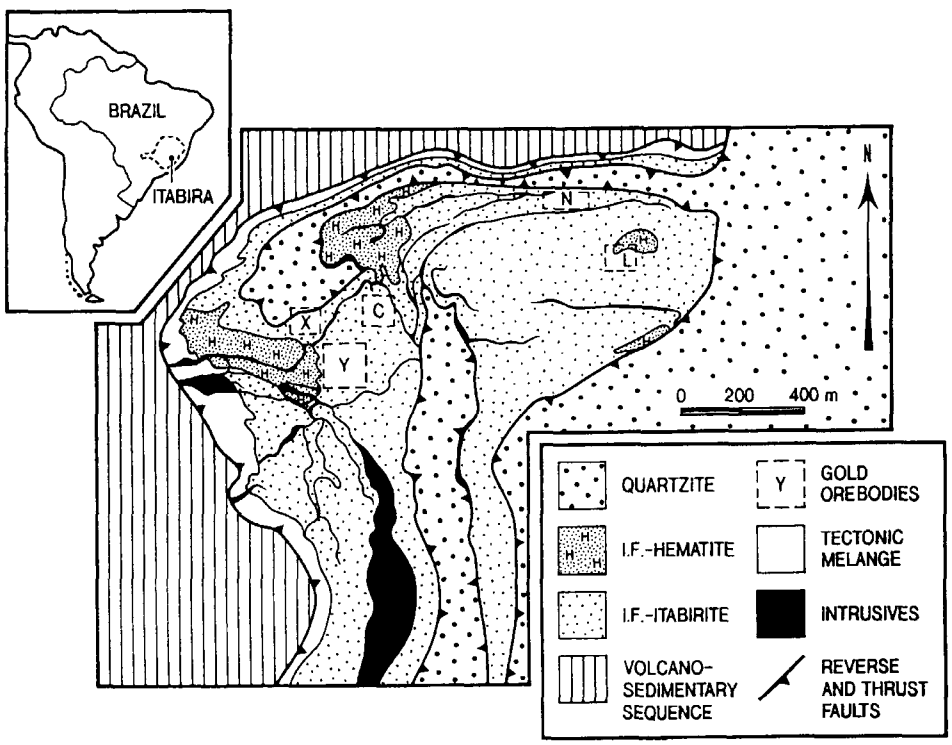

FIG. 1. Simplified geologic map of the Cauê iron mine, Itabira District, Minas Gerais State, Brazil, showing the gold orebodies (C= Central; L= Aba Leste; N= Aba Norte; X= Corpo X; Y= Corpo Y). Modified after Leao de Sá and Borges (1991).

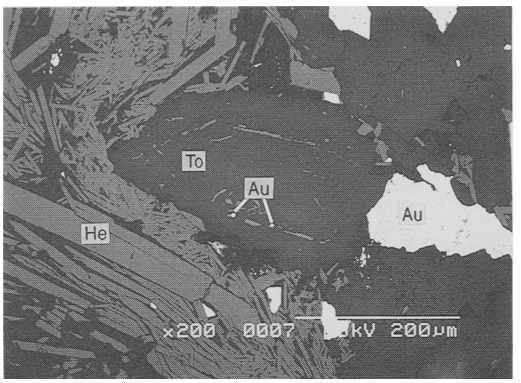

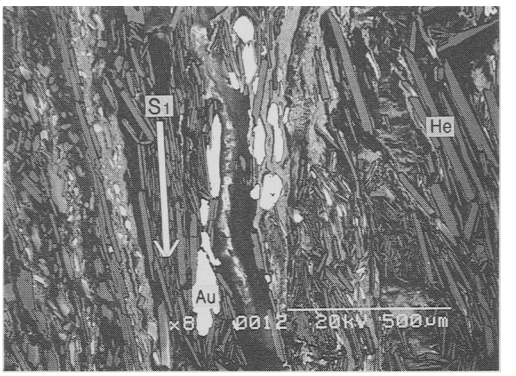

FIGS. 2 and 3. Back-scattered electron images. FIG. 2 (*left*) Gold (Au) as free grains or inclusions in rotated tourmaline (To) in the core of a dismembered sheath fold. He = hematite. FIG. 3 (*right*). Gold (Au) in hematite (He) bands parallel to the S1 mylonitic foliation (from Corpo Y).

tion. The Corpo Y, Corpo X, Central and Aba Leste orebodies are palladium bearing, whereas in the Aba Norte orebody, gold grains have trace contents of rhodium. The Central and the Aba Norte orebodies are not discussed in this paper because gold from Aba Norte is not palladium bearing, and although palladium contents in gold from the Central orebody reach up to 20% (Andrade, priv. comm.), no gold-bearing polished sections were available for textural studies.

Electron-microprobe (EMP) and scanning electron microscope (SEM) analytical techniques

Analyses of polished sections were carried out using the Cameca Camebax automated wavelength-dispersive electron-microprobe (EMP) at McGill University. Calibration for the analyses performed at McGill was done using pure metals, at 20 kV and 20 nA, and analytical precision is better than 0.2%. Energy-dispersive system (EDS) analyses were done for disaggregated gold grains that could not be polished.

Textural and compositional studies were undertaken with the Hitachi S-2300 scanning electron microscope, using a backscattered-electron detector and energy-dispersive spectrometer (EDS) at the Université du Québec à Montréal. Elemental abundances stated here are all in weight percent.

Occurrences of palladian gold

Palladian gold from the Corpo Y orebody is hosted by jacutinga which comprises millimetric to centimetric bands of various concentrations of quartz (± feldspar), hematite (± goethite) and white phyllosilicates, with minor amounts of tourmaline, apatite, and monazite. Carbonate is common as inclusions in quartz grains.

Palladian gold in jacutinga occurs as: (1) free grains and inclusions in rotated tourmaline (Fig. 2) hosted by hematite bands located in the core of dismembered sheath folds; (2) free grains in S1 mylonitic foliation planes of hematite bands (Fig. 3); (3) grains stretched parallel to the ENE elongation lineation (Fig. 4); (4) free grains or inclusions in boudinaged quartz bands; and (5) transposed free grains in S2 foliation planes.

SEM and EMP analyses of gold grains from polished sections of jacutinga show that the palladium contents vary from 1 to 5% (Table 1) and that the highest concentrations are associated with small (commonly smaller than 10 µm) inclusions of Pd–Cu oxides, showing island-mainland and replacement (relict) textures (Figs. 5, 6, and 7), as defined by Ineson (1989). Some

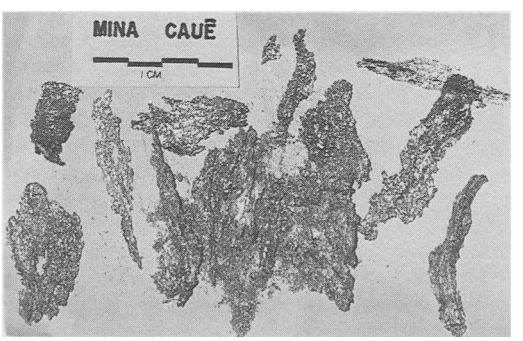

FIG. 4. Gold grains from Corpo Y stretched parallel to the elongation lineation.

TABLE 1. Wavelength-dispersive electron microprobe (EMP) analyses of palladian gold from polished sections of jacutinga, Corpo Y orebody

SAMPLE	Au	Pd	Cu	Ag	TOTAL %
Cau1 (%)	97.36	1.92	0.06	0.27	99.61
(atomic proportion)	0.9584	0.0349	0.0018	0.0049	
Cau2a (%)	90.33	4.54	2.75	0.51	98.13
(atomic proportion)	0.8348	0.0777	0.0788	0.0087	
Cau2b (%)	90.39	4.61	2.98	0.59	98.6
(atomic proportion)	0.8271	0.0781	0.0846	0.0099	
Cau2c (%)	84.37	5.24	8.28	0.14	98.03
(atomic proportion)	0.7029	0.0808	0.2139	0.0021	
Cau5 (%)	92.43	1.83	4.07	0.52	98.85
(atomic proportion)	0.8451	0.0309	0.1153	0.0087	
B2(%)	94.37	1.02	3.1	1.12	99.61
(atomic proportion)	0.8744	0.0176	0.0891	0.019	
B3 (%)	96.11	1.97	0.37	0.69	98.14
(atomic proportion)	0.9409	0.0357	0.0111	0.0123	
Bpa1 (%)	99.12	1.16	0.04	0.09	100.41
(atomic proportion)	0.9761	0.212	0.0011	0.0016	
Bpa3 (%)	97.93	1.2	0.31	0.1	99.54
(atomic proportion)	0.9664	0.0219	0.0094	0.0018	
Bau1 (%)	97.39	1.45	0.11	0.24	99.19
(atomic proportion)	0.9656	0.0265	0.0034	0.0043	
Bau2 (%)	97.76	1.47	0.35	0.38	99.96
(atomic proportion)	0.97761	0.0266	0.0105	0.0069	
Bau3 (%)	97.35	1.4	0.3	0.31	99.36
(atomic proportion)	0.9596	0.0256	0.0091	0.0057	
Bau4 (%)	97.06	1.23	0.58	0.47	99.34
(atomic proportion)	0.9517	0.0223	0.0177	0.0083	
Bau5 (%)	93.35	1.14	3.81	0.79	99.09
(atomic proportion)	0.8587	0.0193	0.1086	0.0133	
Bau6 (%)	97.52	1.26	0.17	0.37	99.32
(atomic proportion)	0.965	0.0231	0.0053	0.0067	
Bau8 (%)	98	1.25	0.1	0.19	99.54
(atomic proportion)	0.9707	0.0228	0.0031	0.0034	

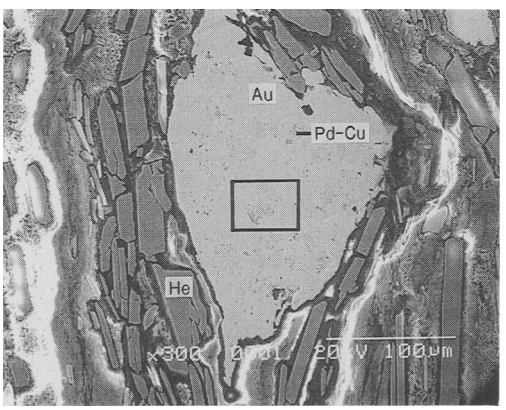

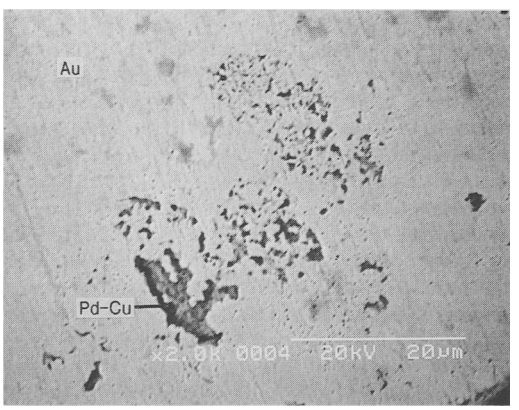

FIGS. 5 and 6. FIG. 5 (*left*) Back-scattered electron image of gold with small inclusions of Pd–Cu oxides, showing island-mainland and replacement (relict) textures (from Corpo Y). FIG. 6 (*right*) Enlargement of area outlined in Fig. 5 showing Pd–Cu oxide inclusions in the gold grain.

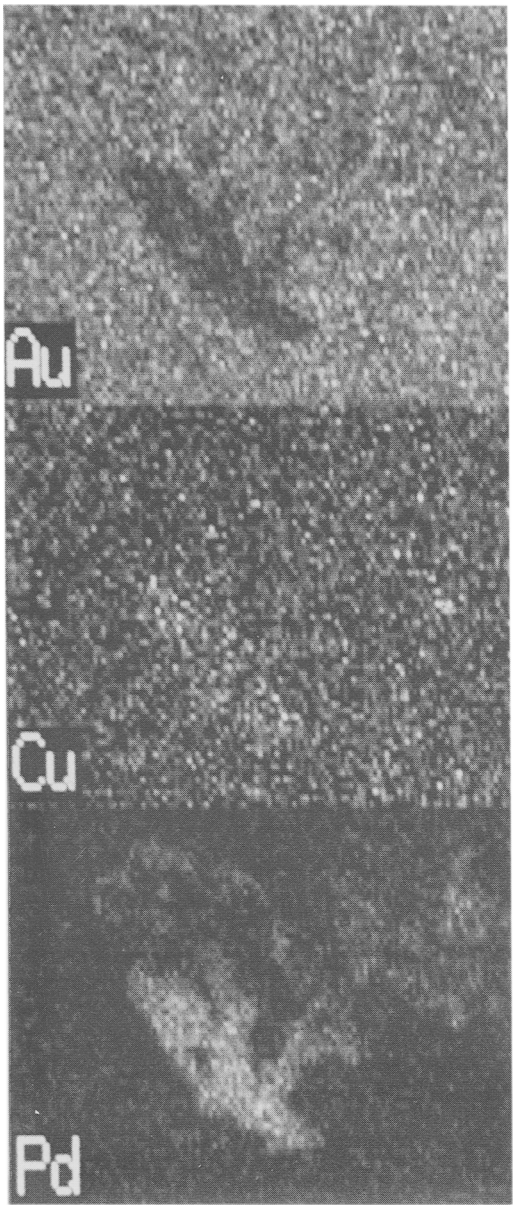

FIG. 7. Single-element scans for Pd, Cu, and Au in the area analysed (enclosed in box) in Fig. 6.

disaggregated gold grains were analysed using an energy-dispersive spectrometer (EDS), revealing palladium contents of up to 20%. Although copper is predominantly concentrated in palladium inclusions, it also occurs directly in gold (Fig. 7), and may reach total contents of 8% (Table 1). Gold grains also contain trace amounts

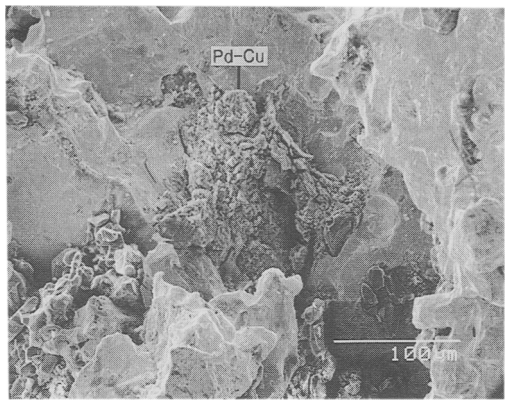

FIG. 8. Scanning electron micrograph of gold grain from Corpo X orebody with a Pd-Cu-oxide inclusion.

of Ag (commonly less than 1%, Table 1) and enclose euhedral inclusions of hematite and tourmaline.

Disaggregated gold grains with high Pd concentrations have a whitish colour and reduced malleability and ductility relative to pure gold.

Corpo X

Palladian gold from the Corpo X orebody occurs in medium- to coarse-grained yellow quartz concentrations hosted by 100–250cm-wide, hematite-rich bands in the jacutinga. Some gold grains, obtained by gravimetric concentration of disaggregated primary ore, are flattened or bent, and contain Pd–Cu oxide inclusions (Figs. 8 and 9). Although copper is more concentrated in palladium inclusions, as in Corpo Y, it is also independently alloyed with gold (Fig. 9). Semi-quantitative analyses using the EDS gave Pd contents of up to 10 %. Inclusions of Cr-bearing hematite and aluminosilicates are observed in a few gold grains.

Aba Leste

Palladian gold from Aba Leste occurs in jacutinga composed of hematite and white phyllosilicates. In polished thin sections, only grains smaller than 20 µm were found. They occur as inclusions in S1-oriented hematite and as free grains in S1 surfaces. Regrettably, the quality of polish was inadequate for quantitative analysis these grains. Palladian gold grains obtained by gravimetric concentration of disaggregated, rich primary ore are flat (Fig. 10) and contain up to 7% Pd (estimated by EDS). Palladium in these gold grains is not related to local concentrations of small inclusions; rather, it

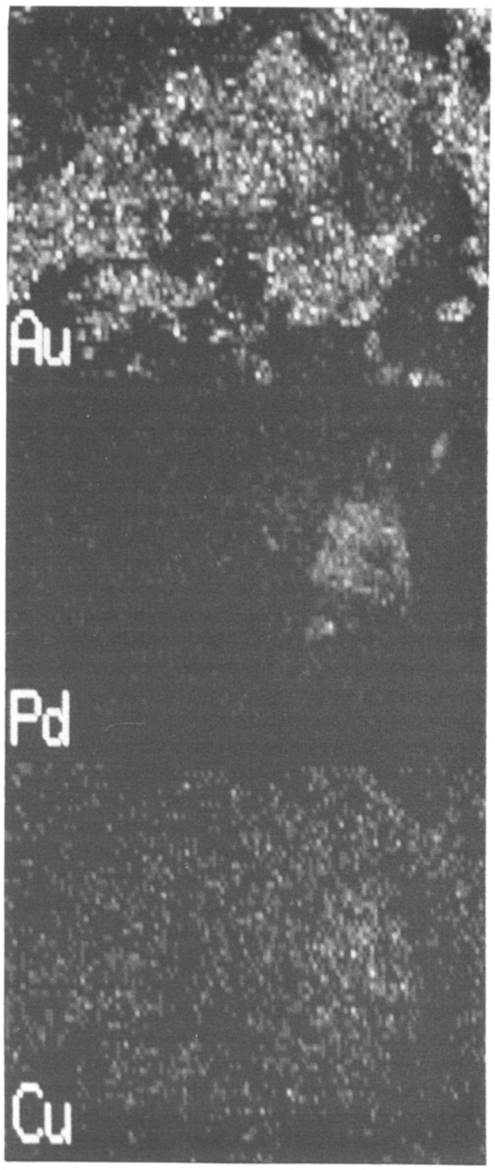

FIG. 9. Single-element scans for Au, Pd, and Cu of the gold grain close to the Pd-Cu-oxide inclusion in Fig. 8.

is homogeneously distributed throughout the gold grains (Fig. 11) a few of which contain Cr-bearing hematite and tourmaline inclusions.

Discussion

Timing of palladium-gold mineralisation

In the three orebodies, palladium-gold mineralization was synchronous with the development of D1-structures.

In Corpo Y, Pd–Cu oxides may have been deposited early during the generation of the S1-mylonitic foliation. It may also have been replaced by gold during progressive deformation: an interpretation based on the presence of small inclusions of Pd–Cu oxides (1) in gold grains stretched parallel to S1, showing island-mainland and replacement (relict) textures; and (2) on slightly stretched gold grains in S1-planes showing replacement textures (Figs. 5 and 6). The second interpretation suggests that replacement in these grains occurred late during the creation of S1 because, if the replacement of Pd–Cu oxides by gold had occurred in the early stages of S1 generation, the gold would have been stretched due to its high ductility.

In Corpo X, replacement of Pd–Cu minerals may also have been synchronous with development of the S1-mylonitic foliation, as indicated by Pd–Cu oxide inclusions in flattened and bent gold grains.

In Aba Leste, palladium is homogeneously distributed in gold grains, suggesting that palladium and gold were deposited contemporaneously during the generation of the S1-mylonitic foliation.

Temperature and oxygen fugacity conditions

Generation of the S1 mylonitic foliation was synchronous with the regional peak of thermal metamorphism which, based on oxygen isotope studies of hematite and quartz (Hoefs *et al.*, 1982), reached approximately 600°C. If the palladium–gold mineralization and the development of D1-structures were coeval, these metals were probably transported at temperatures of at least 600°C and deposited at temperatures of up to 600°C in the iron-formation unit.

Oxygen fugacities during transport and deposition of these noble metals in the iron-formation were probably high, i.e. in the hematite stability field (f_{O_2} higher than 10^{-14} at 600°C; Lindsley, 1976), consistent with the hematitic composition of the host lithology.

Transport and probable mechanisms of deposition of palladium and gold in jacutinga

At high temperatures and oxygen fugacities, Au and Pd may be transported as chloride complexes (Henley, 1973; Seward, 1984; Mountain and Wood, 1988; Gammons *et al.*, 1992), and the dissolution of Au and Pd as chloride complexes

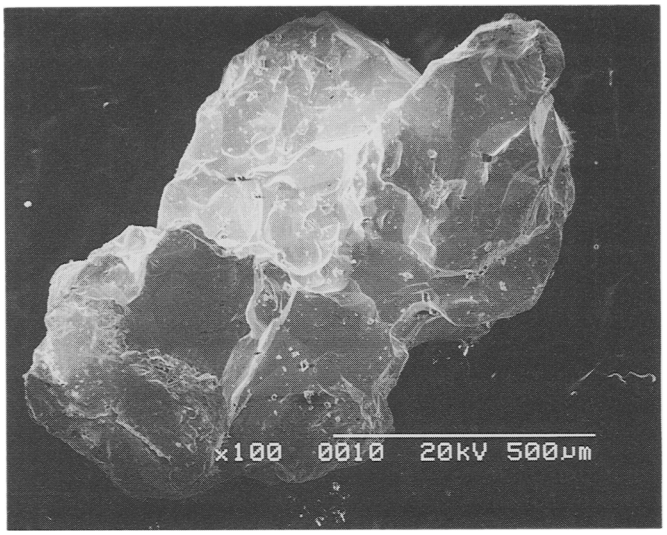

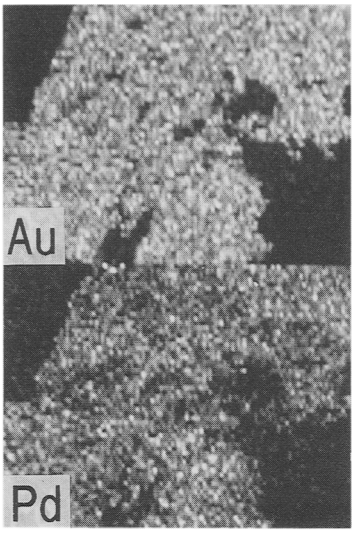

FIG. 10 (*left*) Scanning electron micrograph of a palladian gold grain from Aba Leste. FIG. 11 (*right*) Single-element scans for Au and Pd of the gold grain in Fig. 10.

may be generalized, respectively as:

$$Au\ (s) + \tfrac{1}{2}O_2 + 2H^+ + 2nCl^- = 2AuCl_n^{1-n} + H_2O \quad \text{(r-1)},$$

$$Pd_{(s)} + \tfrac{1}{2}O_2 + 2H^+ + nCl^- = PdCl_n^{2-n} + H_2O_{(l)} \quad \text{(r-2)}$$

In the Cauê mine, high oxygen fugacities and temperatures, as noted by Hoefs *et al.* (1982) and in this study, probably provided favourable conditions for transporting palladium and gold as chloride complexes as discussed above. In this case, deposition of the metals may have occurred in response to an increase in pH (Seward, 1984; Wood and Mountain, 1991). This phenomenon may have occurred as a result of mineralizing fluids reacting with the jacutinga, representing possibly an altered dolomitic itabirite (Dorr and Barbosa, 1963). The presence of (Ca-Fe-Mg-bearing) carbonate inclusions in quartz within the jacutinga may indicate that carbonate was present in the rock matrix and might have reacted with acidic mineralizing fluids, causing an increase in pH according to:

$$Ca(Fe, Mg)(CO_3)_2 + \tfrac{1}{2}O_2 + 4H^+ = 2H_2O + 2CO_2 + Ca^{2+} + (Fe, Mg)^{2+} \quad \text{(r-3)}$$

According to Wood and Mountain (1991) and Gammons *et al.* (1992), palladium concentrations must decrease by two orders of magnitude for each unit increase in the actual pH if the dominant solution species are chloride complexes (see r-2). The same effect can be applied to gold (see r-1). Consequently, a pH increase caused by mineralizing fluids reacting with carbonate-bearing horizons may have been an effective mechanism for depositing gold and palladium. Another mechanism that may also account for the deposition of these metals is the decrease in ΣCl content caused by the dilution of hydrothermal fluids reacting with host rocks (Seward, 1984). In addition, Pd deposition can occur due to saturation with insoluble minerals such as Se-minerals (Mountain and Wood, 1988; Wilde *et al.*, 1989; Gammons *et al.*, 1992). This last mechanism could explain why Pd was deposit earlier than gold, in agreement with the presence of the Pd-Se mineral, palladseite, coated by gold, in bands parallel to S1 (Olivo and Gauthier, 1993).

Conclusions

Although palladian gold occurs in several geological environments, palladium-bearing high-grade gold ore of the Cauê mine provides an excellent opportunity to compare the precious metal mineralogy with the various mechanisms that have been postulated for the genesis of this special type of deposit. From this study, we may conclude that:

(1) palladium and gold mineralization was synchronous with the development of intense

D1-strain features. In Corpo Y and Corpo X, palladium may have been deposited early during the formation of the S1-mylonitic foliation, and replaced by gold during progressive deformation. This conclusion is based on the presence of small inclusions of Pd–Cu oxides in gold grains slightly to completely stretched parallel to S1, showing island-mainland and replacement (relict) textures. In Aba Leste, palladium and gold may have been deposited simultaneously as suggested by the homogeneous distribution of Pd in gold grains; (2) at high oxygen fugacities (hematite stability field) and high temperatures (up to 600°C), as indicated by the oxygen isotope studies and mineralogical assemblage in the auriferous iron-formation, Pd and Au may have been transported as chloride complexes and deposited mainly as a result of changes in pH. Dilution of Cl concentrations may have been a complementary mechanism of Pd and Au deposition, and the deposition of Pd as selenide minerals may have taken place early during the generation of S1-mylonitic foliation.

Acknowledgements

G. R. Olivo gratefully acknowledges receipt of a Conselho Nacional de Desenvolvimento Científico e Regional (CNPq), Brazil, graduate scholarship. Special thanks are extended to the geological staff and management of the Companhia Vale do Rio Doce (CVRD) in the Itabira and Belo Horizonte Districts for field work support, and Glenn Porrier (McGill) and Raymond Mineau (UQAM) for assistance during EMP and SEM analyses, respectively. We are also grateful to L. Harnois for helpful evaluation of the manuscript, C. L. Jenkins for improving the English, and M. Laithier for drafting the figures. This work was partly supported by Quebec Government FCAR funding.

References

Bensusan, A. J. (1929) Auriferous jacutinga deposits. *Inst. Mining. Metall. Bull.*, **8**, 300, 1–25.

Cabri, L. J. (1981) Analyses of Minerals containing platinum-group elements. In *Platinum-Group Elements: Mineralogy, Geology, Recovery* (Cabri, L .J., ed.). Canad. Inst. Mining. Metall. Spec. Vol. **23**, 151–73.

Cabri, L. J. and Laflamme, J. H. G. (1974) Rhodium, platinum, and gold alloys from the Stillwater complex. *Canad. Mineral.*, **12**, 399–403.

Cabri, L. J. and Laflamme, J. H. G. (1979) Mineralogy of samples from the Lac-des-Iles area, Ontario. *Canada Centre for Mineral and Energy Technology, report*, **79–27**, 20 pp.

Clark, A. M. and Criddle, A. J. (1982) Palladium minerals from Hope's Nose, Torquay, Devon. *Mineral. Mag.*, **46**, 371–77.

Dorr, J. V. N.,II, and Barbosa, A. L. M. (1963) Geology and ore deposits of the Itabira district, Minas Gerais, Brazil. *U. S. Geol. Surv. prof. pap.*, **341C**, 110pp.

Gammons, C. H., Bloom, M. S. and Yu, Y. (1992) Experimental investigations of the hydrothermal geochemistry of platinum and palladium: I. Solubility of platinum and palladium sulfide minerals in $NaCl/H_2SO_4$ solutions at 300°C. *Geochim. Cosmochim. Acta*, **56**, 3881–94.

Henley, R. W. (1973) Solubility of gold in hydrothermal chloride solutions. *Chem. Geol.*, **11**, 73–87.

Hoefs, J., Muller, G., and Schuster, A. K. (1982) Polymetamorphic relations in iron ores from Iron Quadrangle, Brazil: the correlation of oxygen isotope variations with deformation history. *Contrib. Mineral. Petrol.*, **79**, 241–51.

Ineson, P. R. (1989) *Introduction to practical ore microscopy*. Longman Earth Science Series, John Wiley & Sons, Inc., New York, 181 pp.

Ladeira, E. A. (1991) Genesis of gold in Quadrilátero Ferrífero: a remarkable case of permanency, recycling and inheritance – a tribute to Djalma Guimaraes, Pierre Routhier and Hans Ramberg. In *Proceedings of Brazil Gold '91: an international symposium on the geology of gold* (Ladeira, E. A., ed.), A. A. Balkema, Rotterdam, 11–30.

Leao de Sá, E. and Borges, N. R. A. (1991) Gold mineralization in Cauê and Conceiçao iron ore mines, Itabira-MG. *Field guide book of Brazil Gold '91: An international symposium on the geology of gold.* (Fleisher, R., Grossi Sad, J. H., Fuzikawa, K., Ladeira, E. A., eds.), 74–85.

Lindsley, D. H. (1976) Experimental studies of oxide minerals. In *Mineralogical Society of America short course notes* (Rumble, D., III, ed.), **3**, L61–L88.

Meireles, E. M. and Silva, A. R. B. (1988) Depósito de ouro de Serra Pelada, Marabá, Pará. In *Depósitos Minerais do Brasil* (Schobbenhaus, C. and Coelho, C. E. S., eds.), **3**, 547–57.

Mountain, B. W. and Wood, S. A. (1988) Chemical controls on the solubility, transport, and deposition of platinum and palladium in hydrothermal solutions: a thermodynamic approach. *Econ. Geol.*, **83**, 492–510.

Olivo, G. R. and Gauthier, M. (1993) Mineralogy of the palladium-bearing gold deposit hosted by a Lake Superior type iron-formation, Cauê Mine, Sao Francisco Craton, Brazil. In *Geological Society of America Annual Meeting. Boston. MA. October 25–28-Abstracts with Programs*, A-276.

Olivo, G. R., Gauthier, M., Bardoux, M., Leao de Sá, L., Borges, N., and Santana, F. C. (1993) Palladium-bearing gold deposits hosted by a Proterozoic Lake Superior-type iron-formation, Itabira Iron District, Minas Gerais, southeast Brazil. *Geological Association of Canada and Mineralogical Association of Canada Joint Annual Meeting. May 17–19. Edmonton. Program and Abstracts*, A-79.

Polônia, J. C. and Souza, A. M. S. (1988) 0 comportamento em microescala do ouro no minério de ferro de Itabira, Minas Gerais. In *Anais do Congresso Brasileiro de Geologia*, **35**, 58–69.

Seward, T. M. (1984) The transport and deposition of gold in hydrothermal systems. In *Proceedings of the Symposium Gold'82: the geology, geochemistry and genesis of gold deposits*. (Foster, R. P., ed.). A. A. Balkema, Rotterdam, 165–81.

Wilde, A. R., Bloom, A. S. and Wall, V. J. (1989) Transport and deposition of gold, uranium and platinum-group elements in unconformity-related uranium deposits. *Econ. Geol. Monogr.*, **6**, 637–60.

Wood, S. A. and Mountain, B. W. (1991) Hydrothermal solubility of palladium in chloride solutions from 300°C to 700°C: preliminary experimental results – a discussion. *Econ. Geol.*, **86**, 1562–3.

[*Manuscript received 13 December 1993: revised 21 February 1994*]